

# Observation of three-dimensional Fermi surfaces in transition-metal chalcogenides/pnictides with orbital fluctuations and superconductivity

T. Mizokawa<sup>1,2\*</sup>

<sup>1</sup> Department of Complexity Science and Engineering, University of Tokyo, 5-1-5 Kashiwanoha, Chiba 277-8561, Japan

<sup>2</sup> Department of Physics, University of Roma "La Sapienza", Piazzale Aldo Moro 2, 00185 Roma, Italy

## 1 Introduction

IrTe<sub>2</sub> consists of Ir triangular lattice layers and exhibits a unique charge orbital order below 275 K [1,2]. With Pt substitution for Ir, the charge-orbital order collapses and an exotic superconducting state is induced [3]. The interesting interplay between the charge-orbital order and the superconductivity has been attracting great interest. In addition, the large spin-orbit interaction in the Ir 5d and Te 5p orbitals is expected to provide a “topological” nature to the multi-band electronic states. In this context, it is highly interesting and important to study the multi-band electronic structure of Ir<sub>1-x</sub>Pt<sub>x</sub>Te<sub>2</sub> by means of angle-resolved photoemission spectroscopy (ARPES).

In this research, we focus on Ir<sub>1-x</sub>Pt<sub>x</sub>Te<sub>2</sub> and related transition-metal chalcogenides or pnictides including Ca<sub>10</sub>(Ir<sub>4</sub>As<sub>8</sub>)(Fe<sub>2-x</sub>Ir<sub>x</sub>As<sub>2</sub>)<sub>5</sub> which consists of metallic Ir-As layer and superconducting Fe-As layer [4].

## 2 Experiment

The ARPES measurements were performed at beam line 28A of Photon Factory, KEK using a SCIENTA SES-2002 electron analyzer with circularly polarized light. The total energy resolution was set to 20-30 meV for the excitation energies from  $h\nu = 40$  to 80 eV. The base pressure of the spectrometer was in the 10<sup>-9</sup> Pa range. The single crystal samples of Ir<sub>1-x</sub>Pt<sub>x</sub>Te<sub>2</sub> ( $x=0.05$ ) and Ca<sub>10</sub>(Ir<sub>4</sub>As<sub>8</sub>)(Fe<sub>2-x</sub>Ir<sub>x</sub>As<sub>2</sub>)<sub>5</sub> were cleaved *in situ* at 20 K and 40 K, respectively, in order to obtain clean and flat surfaces. The cleavage surface is parallel to the IrTe<sub>2</sub> triangular lattice layers for Ir<sub>1-x</sub>Pt<sub>x</sub>Te<sub>2</sub> and to the Ir-As and Fe-As layers for Ca<sub>10</sub>(Ir<sub>4</sub>As<sub>8</sub>)(Fe<sub>2-x</sub>Ir<sub>x</sub>As<sub>2</sub>)<sub>5</sub>.

## 3 Results and Discussion

Figure 1 shows the second derivative plots of the ARPES data as functions of the in-plane momentum  $k_x$ , which is perpendicular to the nearest neighbor Ir-Ir bond direction of the Ir triangular lattice. The band dispersions measured at  $h\nu = 76$  eV (54 eV) approximately correspond to those along the  $\Gamma$ -K (A-H) of the three dimensional Brillouin zone. As shown in Fig. 1(a), a hole band crosses the Fermi level forming a large hole-like Fermi pocket around the  $\Gamma$  point. In going from the  $\Gamma$  point to the A point, the hole band gets flat and the hole-like Fermi pocket is divided into several pieces. This result indicate that the Fermi surface geometry strongly depends on the electron momentum  $k_z$ , which is

perpendicular to the Ir triangular lattice plane, although Ir<sub>1-x</sub>Pt<sub>x</sub>Te<sub>2</sub> has the two-dimensional crystal structure [5].

The three-dimensional Fermi surfaces of Ir<sub>1-x</sub>Pt<sub>x</sub>Te<sub>2</sub> are derived from the Te 5p-Te 5p hybridization between the neighboring IrTe<sub>2</sub> triangular lattice layers which is consistent with the prediction of the *ab-initio* calculation [1]. The comparison between the ARPES result and the *ab-initio* calculation shows that the multi-band structure of Ir<sub>1-x</sub>Pt<sub>x</sub>Te<sub>2</sub> is well reproduced by the LDA calculation without band renormalization if the spin-orbit interactions of the Ir 5d and Te 5p orbitals are taken into account. The present work reveals that the importance of the Te 5p orbitals and their spin-orbit interaction for the exotic superconductivity in Ir<sub>1-x</sub>Pt<sub>x</sub>Te<sub>2</sub>.

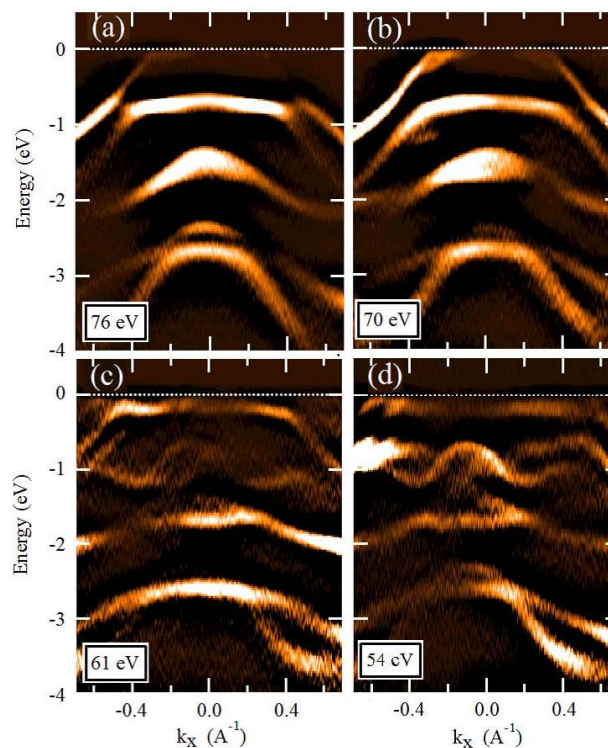


Fig. 1: The multiband dispersions of Ir<sub>1-x</sub>Pt<sub>x</sub>Te<sub>2</sub>( $x=0.05$ ) as functions of  $k_x$  perpendicular to the Ir-Ir bond of the Ir triangular lattice, which are taken at (a)  $h\nu = 76$  eV, (b) 70 eV, (c) 61 eV, (d) 54 eV [5]. The bright belts correspond to the band dispersions.

In addition to the three-dimensional Fermi surfaces and band dispersions of  $\text{Ir}_{1-x}\text{Pt}_x\text{Te}_2$  ( $x=0.05$ ), we have studied the electronic structure of  $\text{Ca}_{10}(\text{Ir}_4\text{As}_8)(\text{Fe}_{2-x}\text{Ir}_x\text{As}_2)_5$ , which has the metallic Ir-As layer in addition to the superconducting Fe-As layer. Figure 2 shows the Fermi surfaces of  $\text{Ca}_{10}(\text{Ir}_4\text{As}_8)(\text{Fe}_{2-x}\text{Ir}_x\text{As}_2)_5$  measured at  $h\nu = 41$  eV (45 eV) approximately correspond to those around the  $\Gamma$  ( $Z$ ) point of the three-dimensional Brillouin zone. The intersection between the three-dimensional Brillouin zone and the  $k_x$ - $k_y$  plane is indicated by the dashed lines which is determined by the periodicity of the Ir-As plane. On the other hand, the two-dimensional Brillouin zone for the Fe-As layer is indicated by the square. The hole-like Fermi pocket is observed at the center of the square and the electron-like Fermi pockets are seen around the corners of the square, as commonly observed in most of the Fe-based superconductors. The observed Fermi pockets can be assigned to the Fe-As plane and are responsible for the superconductivity. In addition, the size of the electron pocket is much larger than that of the hole pocket, indicating that the Fe-As layer is heavily electron-doped.

The ARPES results on  $\text{Ca}_{10}(\text{Ir}_4\text{As}_8)(\text{Fe}_{2-x}\text{Ir}_x\text{As}_2)_5$  have two unique points. Firstly, the Ir 5d band near the Fermi level does not exhibit clear band dispersion or Fermi surfaces, and the lack of the momentum dependence suggests a glassy nature of the Ir-As plane. The glassy nature of the Ir 5d electron would be related to the possible orbital freezing in the Ir-As plane. Secondly, the Fermi surface geometry does not depend on  $k_z$ , which is perpendicular to the Fe-As or Ir-As planes although the metallic Ir-As plane is expected to provide strong hybridization between the layers. Most probably, the glassy or atomically disordered Ir-As layer suppresses the momentum dependent coupling between the Fe-As layers and, consequently, the Fe 3d bands can retain the good two-dimensionality. These results show that the Bloch electrons in the Fe-As layer coexists with the glassy electrons in the Ir-As layer in  $\text{Ca}_{10}(\text{Ir}_4\text{As}_8)(\text{Fe}_{2-x}\text{Ir}_x\text{As}_2)_5$  [6].

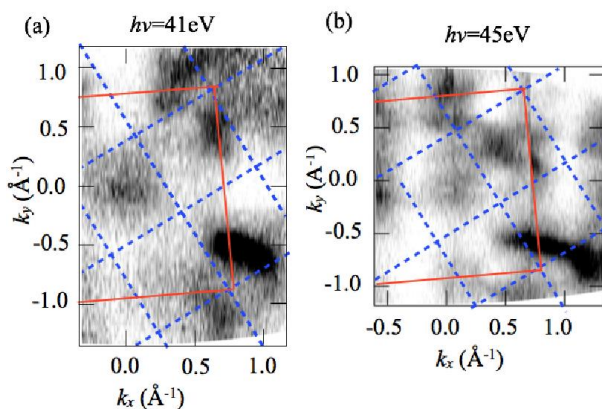


Fig. 2: The Fermi surfaces of  $\text{Ca}_{10}(\text{Ir}_4\text{As}_8)(\text{Fe}_{2-x}\text{Ir}_x\text{As}_2)_5$  as functions of in-plane electron momentum  $k_x$  and  $k_y$ , which are taken at (a)  $h\nu = 41$  eV and (b) 45 eV [6]. The dark regions correspond to the Fermi surfaces.

In summary, by means of ARPES, we have studied the electronic structures of the two exotic superconductors  $\text{Ir}_{1-x}\text{Pt}_x\text{Te}_2$  ( $x=0.05$ ) and  $\text{Ca}_{10}(\text{Ir}_4\text{As}_8)(\text{Fe}_{2-x}\text{Ir}_x\text{As}_2)_5$ . The Ir 5d and Te 5p bands in  $\text{Ir}_{1-x}\text{Pt}_x\text{Te}_2$  ( $x=0.05$ ) strongly depend on the momentum perpendicular to the  $\text{IrTe}_2$  triangular lattice layer, indicating that the Te5p-Te 5p hybridization between the neighboring layers play important roles in the multi-band electronic structure and the superconductivity. On the other hand, the Fermi surfaces of  $\text{Ca}_{10}(\text{Ir}_4\text{As}_8)(\text{Fe}_{2-x}\text{Ir}_x\text{As}_2)_5$  do not appreciably depend on the momentum perpendicular to the Fe-As or Ir-As layers. The ARPES results show that the metallic Ir-As layer is characterized by the strong atomic disorder and a kind of orbital glass state.

#### Acknowledgement

The authors would like to thank K. Horiba, M. Kobayashi, K. Ono, H. Kumigashira for technical supports. Also they acknowledge the collaborations with Mr. D. Ootsuki, Mr. K. Sawada, Mr. T. Sugimoto, Mr. T. Noda, Mr. Y. Chiba, Mr. T. Toriyama, Prof. T. Konishi, Prof. Y. Ohta, Dr. S. Pyon, Prof. K. Kudo, Prof. M. Nohara, Prof. A. Fujimori, and Prof. N. L. Saini.

#### References

- [1] T. Toriyama, M. Kobori, Y. Ohta, T. Konishi, S. Pyon, K. Kudo, M. Nohara, K. Sugimoto, T. Kim, and A. Fujiwara, *J. Phys. Soc. Jpn.* **83**, 033701 (2014).
- [2] G. L. Pascut, K. Haule, M. J. Gutmann, S. A. Barnett, A. Bombardi, S. Artyukhin, D. Vanderbilt, J. J. Yang, S.-W. Cheong, and V. Kiryukhin, *Phys. Rev. Lett.* **112**, 86402 (2014).
- [3] S. Pyon, K. Kudo, and M. Nohara, *J. Phys. Soc. Jpn.* **81**, 053701 (2012).
- [4] K. Kudo, D. Mitsuoka, M. Takasuga, Y. Sugiyama, K. Sugawara, N. Katayama, H. Sawa, H. S. Kubo, K. Takamori, M. Ichioka, T. Fujii, T. Mizokawa, and M. Nohara, *Sci. Rep.* **3**, 3101 (2013).
- [5] D. Ootsuki, T. Toriyama, S. Pyon, K. Kudo, M. Nohara, K. Horiba, M. Kobayashi, K. Ono, H. Kumigashira, T. Noda, T. Sugimoto, A. Fujimori, N. L. Saini, T. Konishi, Y. Ohta, and T. Mizokawa, *Phys. Rev. B* **89**, 104506 (2014).
- [6] K. Sawada, D. Ootsuki, K. Kudo, D. Mitsuoka, M. Nohara, T. Noda, K. Horiba, M. Kobayashi, K. Ono, H. Kumigashira, N. L. Saini, and T. Mizokawa, *Phys. Rev. B* **89**, 220508(R) (2014).

\* mizokawa@k.u-tokyo.ac.jp